



Characterization of Duodenal Microbiota in Patients with Acute Pancreatitis and Healthy Controls

Meng-Qi Zhao^{1,2} · Meng-Yan Cui^{1,2} · Qiao-Li Jiang³ · Jing-Jing Wang¹ · Miao-Yan Fan^{1,2} · Ying-Ying Lu³

Received: 8 December 2022 / Accepted: 4 April 2023 / Published online: 31 May 2023
© The Author(s) 2023

Abstract

Objective The small intestinal bacterial overgrowth (SIBO) in acute pancreatitis correlates with the severity of the disease. However, corresponding studies on the microbial composition of the duodenal mucosa of patients are uncommon.

Methods Duodenal mucosal biopsies were collected by gastroscopy from 16 patients with mild acute pancreatitis (the Ap group) and 16 healthy individuals (the control group) and subjected to histological studies as well as bacterial 16S rRNA gene sequencing. Caerulein and L-arginine were used to induce mild acute pancreatitis (MAP) and severe acute pancreatitis (SAP) in mice, respectively, and their pancreas and duodenum were collected for histological studies.

Results H&E analysis displayed no significant pathological damage in the descending duodenum of patients with acute pancreatitis compared with that of the controls. Immunofluorescence and Real-time PCR revealed that the expressions of tight junction proteins (TJPs) in duodenal mucosa were decreased in acute pancreatitis. The results of the alpha diversity analysis revealed no significant difference between the two groups, while LEfSe and the random forest revealed a few differences, indicating that the descending duodenum mucosal microbiota changed slightly in patients with mild acute pancreatitis. We observed the pathological changes and the expression of TJPs in the duodenum in the three groups of mice and found that SAP mice had more severe pathological damage in the duodenum. Furthermore, the expression of TJPs in the duodenum was lower in the MAP and SAP groups of mice compared to control mice, but it was similar in both groups.

Conclusion Patients with mild acute pancreatitis had mild duodenal barrier dysfunction and slight changes in duodenal mucosal microbiota.

Keywords Acute pancreatitis · Duodenal mucosa · Microbiota · Occludin · ZO-1

Introduction

Acute pancreatitis (AP) often has a moderate and self-limiting clinical course, but in 20–30% of cases, it can escalate to a severe illness with systemic inflammatory response

syndrome SIRS and multiple organ dysfunction syndromes (MODS). Necrotic pancreatic tissue infection with enteric-derived bacteria happens in 30–70% of these patients [1]. These infectious complications are typically the cause of death in patients suffering from acute pancreatitis, with a mortality rate as high as 50% [2–4]. It has been demonstrated that intestinal barrier dysfunction allows bacteria of intestinal origin to transfer to extraintestinal organs, leading to sepsis and subsequent infectious diseases with a high mortality rate [5]. The significance of gut microbiota in the emergence and transmission of critical illnesses is becoming more widely acknowledged.

According to studies, the presence of small intestinal bacterial overgrowth (SIBO) in acute pancreatitis correlates with the severity of the disease [6–8]. SIBO is characterized as bacterial overgrowth in the small intestine caused by an abnormally high number of bacteria and/or changes in the types of bacteria. The authors deem the existence of more

✉ Ying-Ying Lu
le_voyageur@sjtu.edu.cn

¹ Shanghai Key Laboratory of Pancreatic Diseases, Institute of Translational Medicine, Shanghai General Hospital, Shanghai Jiao Tong University School of Medicine, Shanghai, China

² Department of Gastroenterology, Shanghai General Hospital, Shanghai Jiao Tong University School of Medicine, Shanghai, China

³ Department of Gastroenterology, Jiading Branch of Shanghai General Hospital, Shanghai Jiao Tong University School of Medicine, Shanghai 201620, China

than 10^5 bacteria per milliliter of proximal jejunal aspiration to be indicative of SIBO [9]. Although the gold standard for the diagnosis of SIBO is the use of small intestinal fluid bacterial cultures, clinical studies have mostly used portable breath hydrogen concentration meters to measure patients' breath hydrogen concentrations for the diagnosis of intraluminal SIBO [10, 11]. SIBO was found to be more common in MSAP or SAP patients than in MAP patients, and SIBO was linked to organ failure and acute respiratory distress syndrome (ARDS), a complication of acute pancreatitis. Malnutrition, severe malabsorption, and deficiency syndromes can be caused by SIBO. However, it is still unknown how the bacteria in the duodenum change during AP. The response of acute pancreatitis to chemicals in the duodenum is facilitated by neuronal cross-talk between the duodenum and pancreas [12]. Additionally, when the pancreas is dysfunctional, it can cause a decrease in bicarbonate secretion, resulting in the inability of the proximal duodenum to neutralize gastric acid, thus inducing duodenal inflammation [13].

Numerous studies indicate that acute pancreatitis commonly alters the intestinal microbiota and that intestinal microbiota dysbiosis might impair immunological function, increase intestinal permeability, and encourage intestinal bacterial metastasis [14, 15]. It was found through animal experiments that the small intestine may be the main source of intestinal bacteria in infected pancreatic necrosis, rather than the colon [16]. Another study in rats, in which fluorescent bacteria were observed to migrate from the lumen of the small intestine into the pancreas by Intravital microscopy of fluorescent bacteria, provided substantial experimental evidence for the hypothesis of an intestinal origin-pancreatitis infection complication [17]. Similarly, duodenal ecological dysregulation has been found in patients as a potential risk for infection in patients with severe acute pancreatitis [18]. In this study, the examination of the generated metadata by the SourceTracker tool revealed that the duodenum was the most likely source of bacteria that later invaded pancreatic tissue in this model [19]. About 90% of the energy in the meal is absorbed by the small intestine mucosa, which has a large surface area [20]. A sufficient capacity for absorption depends on mucosal integrity, which is continually threatened by the intraluminal environment, including bacteria [21]. Several studies have used animal models to investigate how the gut microbiota changes during acute pancreatitis [22, 23]. Similarly, significant differences in the structure of the gut microbiota between acute pancreatitis and healthy control have been observed in adult participants, and a disordered microbiota is strongly associated with systemic inflammation and intestinal barrier dysfunction. However, these studies only focused on the microbiota in the intestine [15]. There aren't many studies that correspond to the microbial makeup of patients' duodenum. The big duodenal papilla, where the common bile duct and pancreatic duct

exit, brings the duodenum and pancreas closer anatomically. Therefore, we hypothesize that microbiota can pass retrogradely through the pancreatic duct and that duodenal microbiota and infection in pancreatitis may be related. The structural alterations in the duodenal mucosal microbiota in people with acute pancreatitis are the main focus of this investigation.

Materials and Methods

Clinical Trial Design and Sampling

This study examines the differences in intestinal microbiota among acute pancreatitis patients and healthy individuals. It involved 32 patients who underwent a gastroscopy at the Jiading Branch of Shanghai General Hospital (Shanghai) between October 2021 and February 2022. After undergoing a routine physical examination, 16 patients with acute pancreatitis (11 males and 6 women) were assigned to the Ap group. The Ap group was mostly mild to moderate. 16 healthy volunteers (11 males, 6 females, ages 32–58) were assigned to the control group. Abdominal pain was the most prevalent symptom among the 16 individuals with acute pancreatitis, followed by abdominal distension, nausea, and vomiting.

Patients and healthy controls were excluded if they took antibiotics, probiotics, Chinese herbs, steroids, and other substances that may influence the structure of the microbiota up to 8 weeks before sampling. Other exclusion criteria involved patients with a history of gastroscopy intolerance, immunodeficiency, allergy, asthma, celiac disease, colon cancer, diabetes, HIV, inflammatory bowel disease, irritable bowel syndrome, gastroenteritis, narcotic small bowel colitis, and arthritis. Before collecting any samples, all patients provided written informed consent, which was authorized by the research ethics committees of Shanghai General Hospital. Every biochemical analysis was handled by the Shanghai General Hospital Laboratory. After an overnight fast, blood samples were taken on the second day of hospitalization. We collected mucosal biopsy samples that were obtained via gastroscopy from the two groups around the 5th day after diagnosis. Each patient had two duodenal biopsy samples obtained during the upper endoscopy. One tissue sample was frozen immediately and stored at $-80\text{ }^{\circ}\text{C}$, while the other was fixed in 10% formaldehyde in phosphate-buffered saline (PBS; pH 7.4) and embedded in paraffin.

Mice Experimental Design

Shanghai Leagene Biotechnology Co.Ltd (Shanghai, China) provided male C57BL/6 mice weighing 20–22 g. All mice were kept in special pathogen-free (SPF) environments

that had a temperature of 23 ± 2 °C, a 12-h cycle of light and dark, and free access to water and mouse chow. The guidelines of the Animal Care and Use Committee of Shanghai Jiao Tong University were followed in all animal experimentation.

The mice were randomly divided into three groups: healthy control (the CON group), caerulein-induced pancreatitis (the MAP group), and L-arginine-induced pancreatitis (the SAP group) and five mice in each group. Mice in the MAP group were given 100 µg/kg caerulein intraperitoneally every hour for 10 times and mice in the SAP group received two intraperitoneal injections of L-arginine hydrochloride (8%, pH=7.0, 4.5 g/kg) given every 2 h.

Histopathology

Duodenal biopsy tissue samples were immobilized in 4% paraformaldehyde, dehydrated, embedded in paraffin, cut into 4 µm sections, and stained using hematoxylin and eosin (H&E). The morphologic evaluation was performed by a light microscope (Leica, Germany) at a magnification of $\times 200$ according to a modified Chiu's score: Grade 0, normal mucosal villi, no ulceration or tissue damage, and no inflammatory reactions; Grade 1, Limited infiltration of inflammatory cells in the lamina propria and the development of a subepithelial Gruenhagen space, typically at the apex of the villus; Grade 2: diffuse infiltration of inflammatory cells into the lamina propria, extending into the subepithelial space, with moderate epithelial elevation; Grade 3: Subendothelium localized infiltration of inflammatory cells and severe epithelial raising down the sides of the villi; Grade 4, exposed lamina propria and dilated capillaries, as well as a diffuse infiltration of inflammatory cells in the subendothelium; Grade 5, digestion, disintegration, bleeding, and ulceration of the lamina propria along with severe inflammatory reactions [24]. The pancreatic and duodenal specimens were fixed with 4% paraformaldehyde and dehydrated. Then they were embedded in paraffin, cut into 4 µm sections and stained with H&E. A light microscope (Leica, Germany) was used to evaluate the morphology at magnifications of $\times 100$ and $\times 200$. According to Schmidt's criteria, the histological abnormalities in the pancreas, including pancreatic edema, acinar cell necrosis, bleeding, and inflammation, were assessed [25].

Immunofluorescence

Duodenal mucosa sections were heated for 1 h at 60 °C. Next, sections were put in Leica Autostainer XL (Leica, USA) (xylene for 40 min, 100% ethanol for 10 min, 95% ethanol for 10 min, 80% ethanol for 5 min, 70% ethanol for 5 min, and doubly distilled water for 3 min) to deparaffinize and rehydrate the samples. A citrate antigen retrieval

solution was used to extract antigens (Sangon Biotech, China). After washing the tissue several times in phosphate-buffered saline (PBS), a super pap pen (Sangon Biotech, China) was used to draw a circle around it. Slides were incubated with primary antibodies against Occludin and ZO-1 diluted with primary antibody dilution solution (Servicebio, China) for overnight incubation at 4 °C after being blocked for an hour at room temperature with immunostaining blocking buffer (Sangon Biotech, China). The slides were cleaned with PBS and then incubated with Alexa Fluor 488 AffiniPure donkey antirabbit IgG (Yeason, China) for 1 h at room temperature. Then, the slides were rinsed with PBS and dyed with dihydrochloride (Yeason, China) for 10 min. Images were captured with a fluorescence microscope (Leica, USA).

Quantitative Reverse Transcription PCR

Total RNA was extracted from tissues using TRIzol (Invitrogen, USA) and a tissue RNA purification kit plus (EZBioscience, USA). cDNA was synthesized using HyperScript III RT SuperMix for quantitative PCR (qPCR) with genomic DNA (gDNA) remover (EnzyArtisan, China). A NanoDrop2000 equipment (Thermo Scientific, USA) was used to measure the concentration of RNA or DNA. With QuantStudio 6 Flex real-time PCR systems, the real-time PCR was carried out according to the procedure listed below (Thermo Scientific, USA): predenaturation (95 °C for 30 s), 40 amplification cycles of denaturation (95 °C for 10 s), and annealing and extension (60 °C for 30 s). Gene expression was measured by the $2^{-\Delta\Delta CT}$ method. The detection primers are listed in Table S1.

DNA Extraction PCR Amplification and Sequencing of Bacteria in Duodenal Mucosa

Duodenal biopsy tissues were soaked in 20 µl of 20 mg/ml protease solution and 300 µl of PBS solution at 60 °C overnight. The samples were suspended in 790 µl of sterile lysis buffer (4 M guanidine thiocyanate; 10% N-lauroyl sarcosine; 5% N-lauroyl sarcosine-0.1 M phosphate buffer, pH 8.0) in 2 ml screw-cap tube containing 1 g glass beads (0.1 mm BioSpec Products, Inc., USA). After vigorous vortexing, this mixture was incubated for an hour at 70 °C while being forcefully bead beaten for 10 min. The E.Z.N.A.® Stool DNA Kit (Omega Bio-tek, Inc., GA), which skips the lysis steps, was used to extract microbial genomic DNA from the duodenal biopsies in accordance with the manufacturer's instructions and was stored at -20 °C for further analysis. The universal bacterial primers F1 and R2 (5'- CCTACC GGNGGCWGCAG-3' and 5'-GACTACHVGGGTATCTA ATCC-3'), which map to locations 341 to 805 in the Escherichia coli 16S rRNA gene, were used to amplify the V3–V4 region of the bacterial 16S ribosomal RNA gene from each

sample. The following program was used to run PCR reactions in an EasyCycler 96 PCR system (Analytik Jena Corp., AG): 3 min of denaturation at 95 °C, followed by 21 cycles of 0.5 min of denaturation at 94 °C, 0.5 min of annealing at 58 °C, and 0.5 min elongation at 72 °C, with a final 5 min extension at 72 °C. Shanghai Mobio Biomedical Technology Co. Ltd. sequenced the products from various samples using the Miseq platform (Illumina Inc., USA) in accordance with the manufacturer's instructions.

Bioinformatics Analysis of Sequencing Data

USEARCH (version 11.0.667) was used to extract clean data from raw data using the following criteria: (i) Sequences of each sample were extracted with zero mismatches using each index. (ii) Sequences with less than 16 bp overlap were discarded. (iii) Any overlap error rate greater than 0.1 was discarded. (iv) Sequences with less than 400 bp after the merge was removed. Quality-filtered sequences were grouped into distinct sequences and sorted in decreasing abundance using UPARSE in accordance with the UPARSE OTU analysis pipeline, excluding singletons, in order to find representative sequences. Operational Taxonomic Units (OTUs) were classified using UPARSE (version 7.1 <http://drive5.com/uparse/>) and annotated using the SILVA reference database (SSU138) based on 97 percent similarity after chimeric sequences were removed. Mothur v1.42.1 was used to evaluate the Alpha diversity metrics (ACE estimator, Chao 1 estimator, Shannon–Wiener diversity index, and Simpson diversity index). We employed principal coordinates analysis (PCoA) and nonmetric multidimensional scaling (NMDS) plots based on the unweighted UniFrac dissimilarity to depict the structural diversity of the gut microbiome in the discovery group. The statistical significance of beta diversity was assessed using an Adonis analysis. To ascertain whether there were notable variations in microbial composition between groups, a Wilcoxon rank-sum test was utilized. To detect taxa with differential abundance among groups, the linear discriminant analysis (LDA) effect size (LEfSe) method was used (LEfSe version 1.1, <https://github.com/SegataLab/Lefse>). As expected by a random forests model, the microbiome heatmap analysis showed distinct gut microbiomes in both groups. PICRUST2 v2.4.1 was employed to forecast functional abundances based on 16S rRNA gene sequences.

Statistical Analysis

The data were displayed as the mean \pm standard deviation (SD). The Student's *t* test, Mann–Whitney test, and Spearman correlation test were carried out using SPSS 19.0 software, and a *p* value of < 0.05 was considered statistically significant.

Data Availability

The Sequence Read Archive database, accession number PRJNA877061, contains the 16S rRNA gene V3–V4 regions' raw sequencing data as well as the information that goes with it.

Results

Clinical Characteristics

This duodenal mucosal microbial profiling study involved 32 participants. Table 1 summarizes the characteristics of the 16 healthy controls and the 16 patients with acute pancreatitis, including demographics, fasting blood glucose level, blood fat (TC, TG), and plasma inflammatory markers such as CRP, IL-6, WBC, and PCT. Some baseline characteristics, such as age, BMI, PT and blood glucose levels, did not differ significantly between the two groups. However, TC and TG levels were higher in the group of patients with acute pancreatitis. The patient group also had significantly higher levels of CRP, IL-6, WBC, and PCT, indicating an acute inflammatory disease.

Histopathological and Expression Levels of TJPs

Most healthy controls had normal duodenal epithelium and villi, but there were mucosal specimens in the lamina propria that showed mild chronic inflammation. (Fig. 1A). In the duodenum of patients with acute pancreatitis, we found no mucosal damage, villi atrophy, or rupture, but there was more severe hemorrhage and inflammatory cell

Table 1 Baseline characteristics of the individuals enrolled

Variable	Healthy controls (<i>n</i> = 16)	Acute pancreatitis patients (<i>n</i> = 16)	<i>p</i> Value
Age (mean \pm SD)	42.50 \pm 7.16	46.06 \pm 11.18	0.056
Gender			
Female	6 (37.5%)	6 (37.5%)	
Male	10 (62.5%)	10 (62.5%)	
BMI (kg/m ²)	24.69 \pm 2.91	25.67 \pm 3.60	0.618
Glucose (mmol/L)	5.59 \pm 0.81	6.10 \pm 0.92	0.531
WBC ($\times 10^9$)	5.98 \pm 1.15	9.33 \pm 3.43	< 0.05
PLT ($\times 10^9$)	235.69 \pm 45.93	206.31 \pm 45.49	0.833
CRP (mg/L)	6.42 \pm 1.70	65.68 \pm 76.21	< 0.001
IL-6 (pg/mL)	4.96 \pm 2.21	32.57 \pm 33.75	< 0.001
PCT (ng/ml)	0.040 \pm 0.01	0.12 \pm 0.04	< 0.05
PT (s)	12.10 \pm 0.72	12.78 \pm 0.99	0.489
TC (mmol/L)	3.90 \pm 0.80	4.81 \pm 1.30	< 0.05
TG (mmol/L)	1.90 \pm 0.98	2.49 \pm 2.34	< 0.05

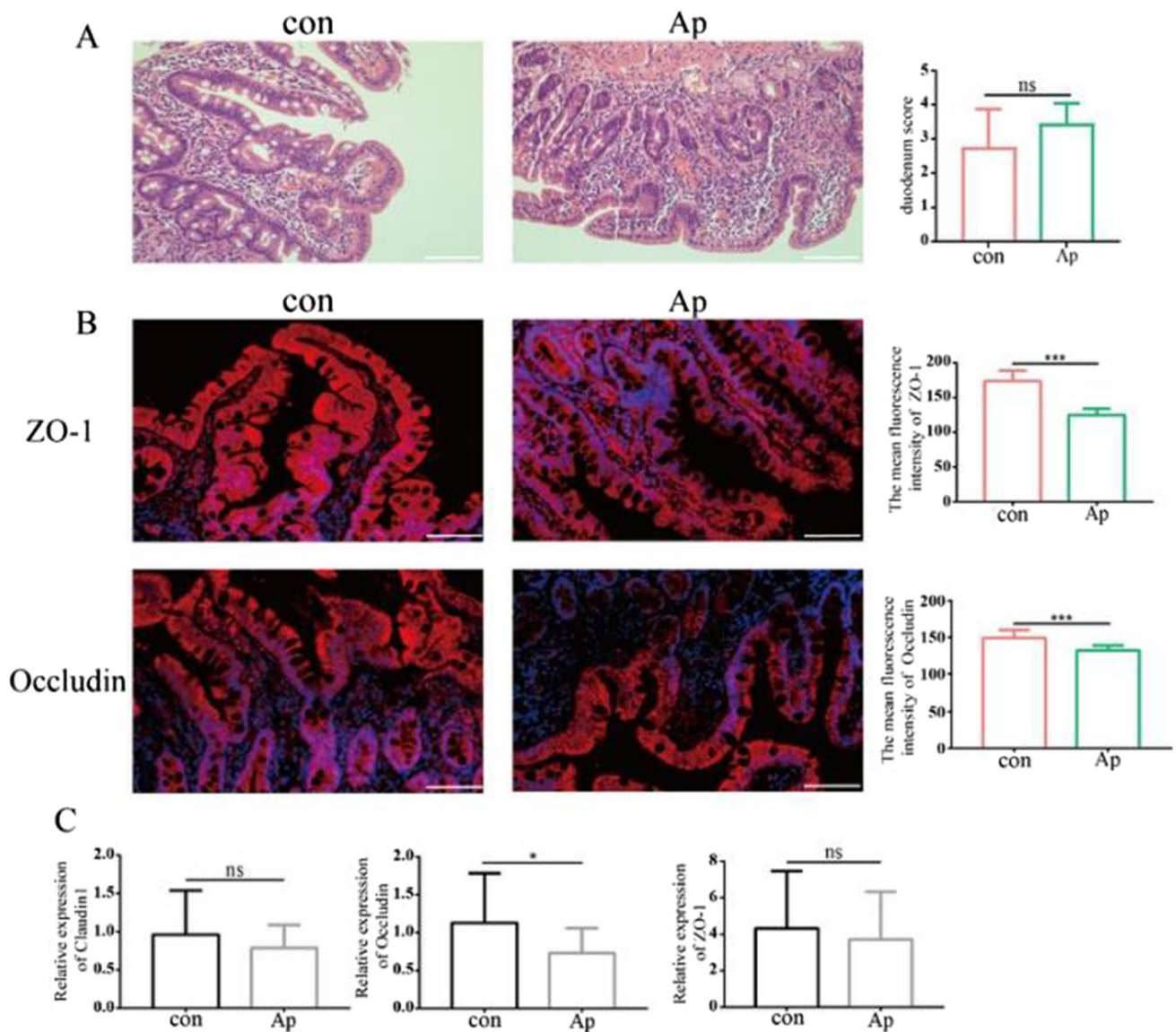


Fig. 1 H&E-stained tissue sections of duodenum and protein and mRNA expression levels of TJPs. **A** The evaluation of intestinal injury with modified Chiu's scores in the two groups. Microscopic images were taken at 200×magnification. Scale bar=50 μm. **B**

Representative images of fluorescence staining of TJPs (red) of the duodenum. **C** mRNA expression levels of TJPs (Claudin1, Occludin and ZO-1). Symbol *means $p < 0.05$, **means $p < 0.01$, ***means $p < 0.001$, ns means $p > 0.05$, Student's *t* test

infiltration. However, when compared to the control group, there were no appreciable variations in the duodenal pathology scores. To determine whether duodenal intestinal permeability had changed, immunofluorescence was used to examine the expression of intestinal TJPs Occludin and ZO-1 in the duodenum of patients with acute pancreatitis. Compared with healthy individuals, the expression of Occludin and ZO-1 decreased in AP individuals slightly, indicating some degradation of the duodenal mucosal barrier in acute pancreatitis (Fig. 1B). By using real-time qPCR, we discovered that the expression of TJPs (Occludin, ZO-1, and Claudin1) was higher in healthy controls

than in patients with acute pancreatitis, with Occludin being statistically significant (Fig. 1C). To verify the duodenal mucosal barrier function at different disease severity, we observed the pathology and TJPs changes in the duodenum of three groups of mice (the CON, MAP and SAP groups). When compared to controls, mice with MAP had some pathological damage to the duodenum, whereas mice with SAP had more severe pathological damage to the duodenum (Fig. S4AB). Furthermore, the expression of TJPs in the mouse duodenum was found to be lower in the MAP and SAP groups compared to control mice, but similar in both groups (Fig. S4C).

MiSeq Sequencing Data Summary and Alpha Diversity Analysis of the Duodenal Bacterial Microbiota

In total, 877,091 usable sequences were obtained from 32 samples using Illumina MiSeq sequencing, with an average of 27,409 sequences per sample. From these, 732 OTUs were identified at a 97% similar level. With the current sequencing, the rarefaction curves achieved a plateau, and the Shannon diversity estimates of all the samples were constant (Fig. S1A, B), suggesting that most diversity had already been captured. According to Venn diagrams, there were 626 OTUs in both groups, with 54 specific to the group of patients with acute pancreatitis and 52 specific to the healthy control group (Fig. 2A). Based on the OTUs observed in each sample and the ACE and Chao indices, which reflect the richness of species diversity, it was discovered that the acute pancreatitis group had fewer OTUs, but the two groups' microbiota diversity and richness did not significantly differ from one another. (Fig. 2B–F).

Analysis of the Beta Diversity Based on OTU Levels

Beta diversity was used to ascertain how samples differed from one another. To compare whether samples had significant microbial community differences, we used the widely used unweighted UniFrac analysis, which was calculated based on evolutionary information between individual sample sequences. Adonis analysis revealed a significant difference in the two groups (Adonis: $p = 0.0169$). Based on the unweighted UniFrac distances, a PCoA also showed that the microbial composition of the Ap group deviated from the control group according to the PC1, which accounts for 17.64%, demonstrating that the overall gut microbiota in the two groups had different bacterial microbiota compositions (Fig. 3A).

Comparison of the Bacterial Microbiota in Healthy Volunteers and Acute Pancreatitis

To further elucidate the differences in microbial structure, we calculated the relative abundance of bacteria. The average relative abundance of microbiomes at the phylum level is represented in Fig. 4A. In the control group, the duodenal mucosal microbiota was dominated by *Proteobacteria*, followed by *Actinobacteriota*, *Firmicutes*, and *Bacteroidota* with proportions of 48.2%, 25.4%, 13.5%, and 9.1%, respectively. *Firmicutes* proliferated while *Proteobacteria* and *Bacteroidetes* decreased when compared with the CON group, but the Wilcoxon rank sum test did not find any significant differences in these bacterial phyla between the two groups. (*Proteobacteria* 43.8%, *Actinobacteriota* 24.6%, *Firmicutes* 22.5% and *Bacteroidetes* 7.1%).

Figure S2A shows the average relative abundance of microbiomes at the class level, the duodenal mucosal microbiota was dominated by *Gammaproteobacteria*, *Actinobacteria*, *Bacteroidia* and *Bacilli* in the control group. The microbiota in the Ap group had a comparable makeup to that in the control group. The average relative abundance of microbiomes at the order level is depicted in Fig. S2B, the composition of both groups was dominated by *Oceanospirillales*, *Corynebacteriales*, *Burkholderiales* and *Propionibacteriales*. In comparison to the control group, the Ap group had a considerably higher concentration of *Lactobacillales*. At the family level, the duodenal mucosal microbiota was dominated by *Halomonadaceae*, *Dietziaceae*, *Idiomarinaceae* and *Nocardiodaceae* (Fig. S2C). *Streptococcaceae* abundance was noticeably higher in the Ap group compared to the control group.

At the genus level, the duodenal mucosal microbiota was dominated by *Halomonas* in the Ap group, followed by *Dietzia*, *Aliidiomarina* and *Aeromicrobium* with proportions of 15.5%, 11.1%, 8.0%, 4.5%, respectively. Similarly, these four species were the dominant genera in the control group, and their proportions were 18.3%, 11.4%, 8.7%, and 8.1% (Fig. 4B). The duodenal mucosal microbiota in the acute pancreatitis group had a higher abundance of *Streptococcus* and *Neisseria*. *Halomonas* and *Achromobacter* were more prevalent in the healthy group than in the Ap group. The Wilcoxon rank sum test indicated that *Actinobacillus* and *Oribacterium* were significantly different in the two groups, and both were more abundant in the healthy tissue (Fig. 4C). Furthermore, we discovered that the abundance of *Actinomyces* and *Oribacterium* was inversely correlated with clinical inflammatory indices in the control and Ap groups, but not statistically different. ($p > 0.05$; Fig. 3S).

Differences in Microbiome Compositions Between the Groups

We performed LEfSe, showing the microbial structure that differed most between patients with acute pancreatitis and healthy controls (Fig. 5A). According to LEfSe analysis at the genus level, *Microtrichales*, *Pseudomonas*, *Ruminococcaceae*, and *Pediococcus* were more abundant in the duodenal mucosa of acute pancreatitis patients. Conversely, the abundances of various genera, including *Bacteria*, *Prevotellaceae*, *Bacilli_RF39*, *Bilophila*, *Candidatus Saccharimonas*, *Treponema*, and *Stomatobaculum*, were significantly higher in the control group than in the Ap group.

It was found that the gut microbiomes of both groups differed using a random forest model (Fig. 5B). There were discovered to be 21 OTUs in all that was different between the two groups. Among these OTUs, 6 OTUs were more abundant in the Ap group than in the control group, belonging to the genera of *Pseudomonas*, *Halomonas*,

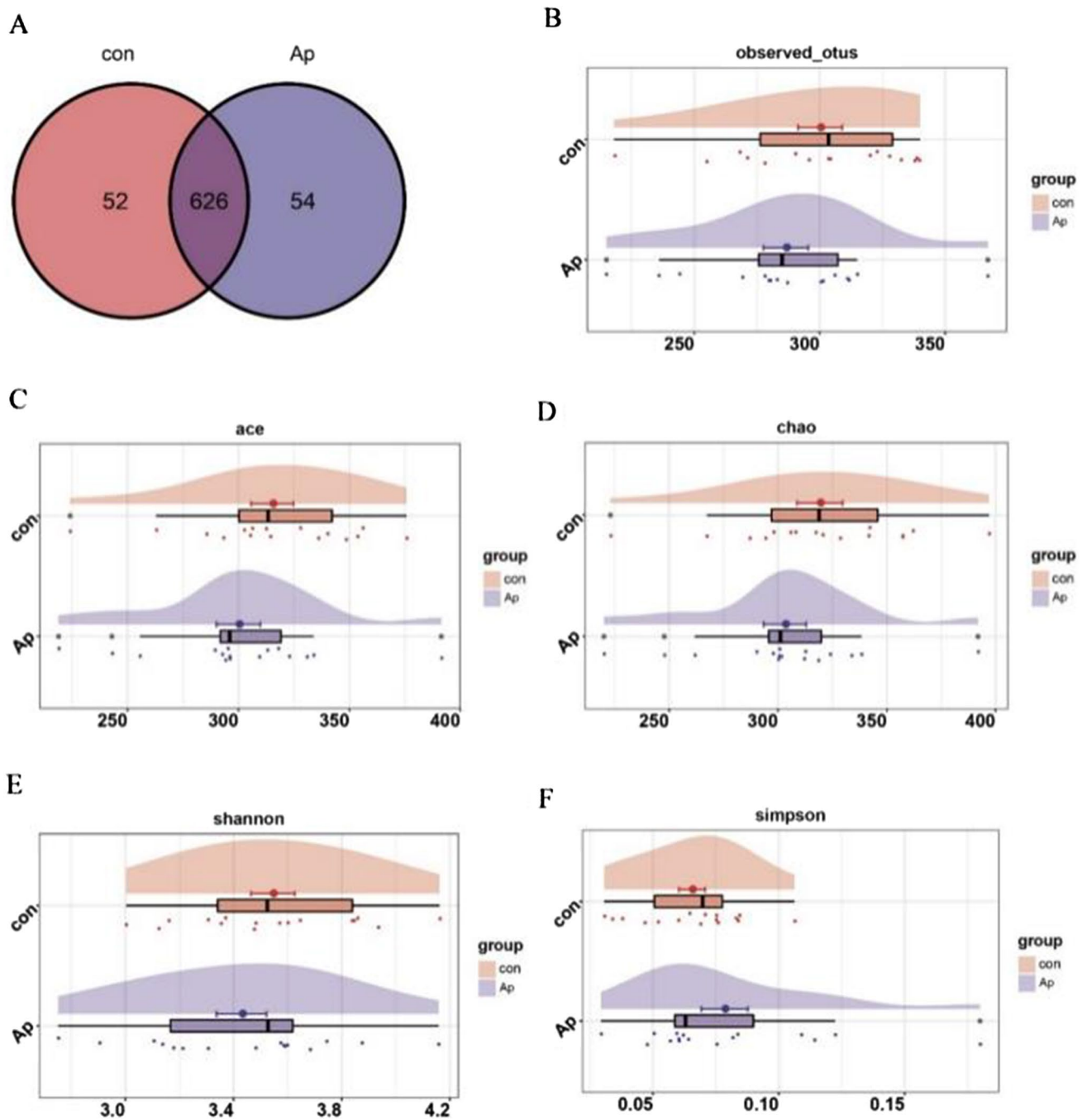


Fig. 2 Operational Taxonomic Units clustering and alpha diversity analysis of the microbiota of the duodenal mucosa. **A** Venn diagram demonstrates the shared and unique Operational Taxonomic Units

(OTUs) in both groups. **B** The OTUs in the single sample from each group. **C–F** The estimators of ACE, Chao, Shannon and Simpson of duodenal bacterial microbiota in each group

Lachnospiraceae_NK4A136_group, *Microtrichales*, *Bacteria*, and *Nesterenkonia*. Correspondingly, OTUs belonging to the genera of *Streptococcus*, *Actinobacillus*, *Haemophilus*, *Prevotellaceae*, *Saccharimonadaceae*, *Candidatus_Saccharimonas*, etc., were more abundant in the control group than in the Ap group.

Functional Alterations of Duodenal Mucosal Microbiota Microbiomes in Both Groups

Based on the KEGG module and KEGG pathway databases, 16S sequencing data was used for functional prediction, and LEfSe was then used to sort the different

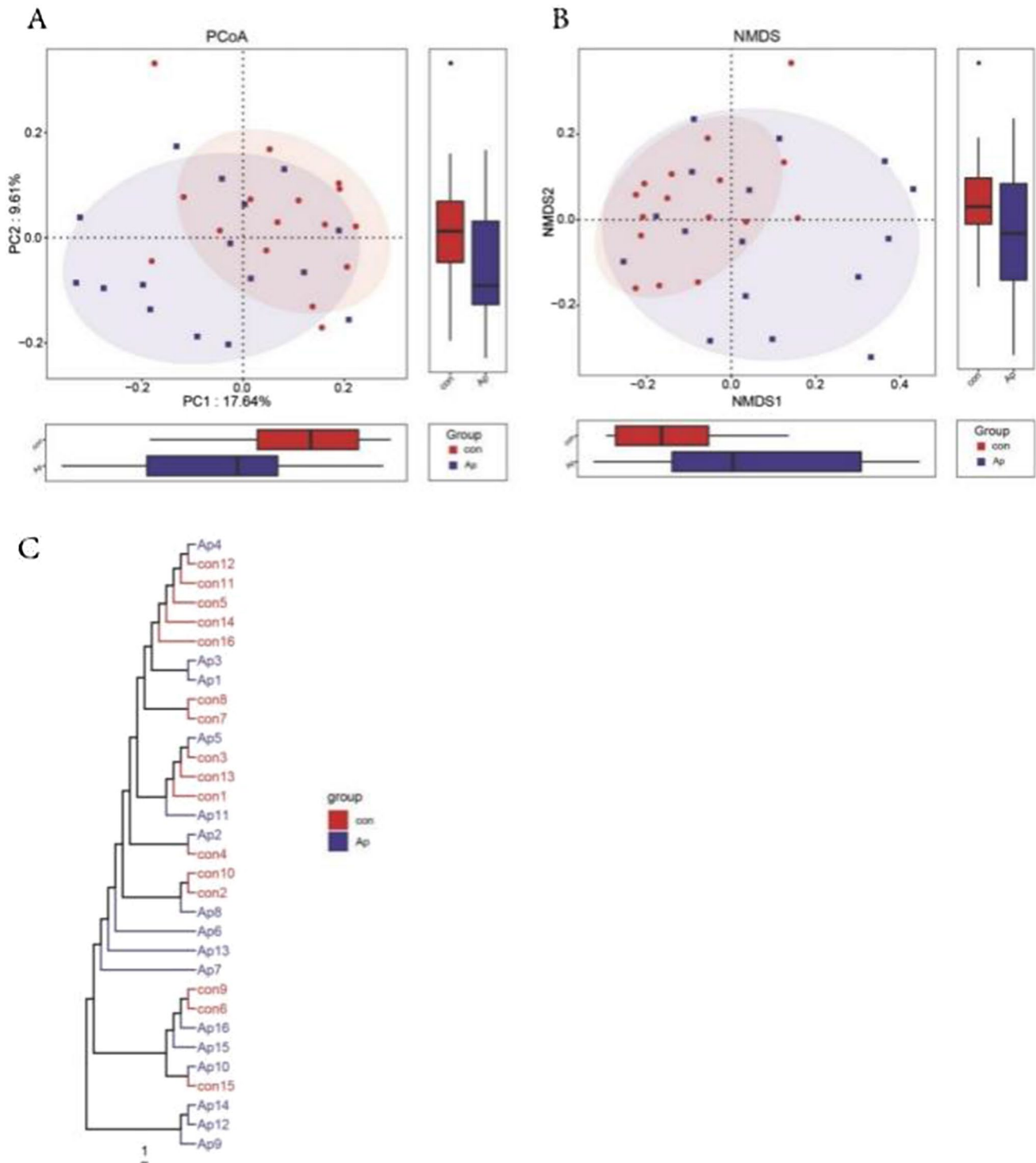


Fig. 3 Analysis of beta diversity of the duodenal mucosa in both groups. **A** Principal coordinates analysis plots based on unweighted UniFrac distances between the two groups. **B** Nonmetric multidimensional scaling analysis plots based on unweighted UniFrac distances between the two groups. **C** Cluster tree between the two groups

healthy individuals. However, ABC_transporters, Glycine_serine_and_threonine_metabolism, Selenocompound_metabolism, Apoptosis,

Endocrine_system, Glycerolipid_metabolism, and Dioxin_degradation were significantly higher in acute pancreatitis individuals compared to

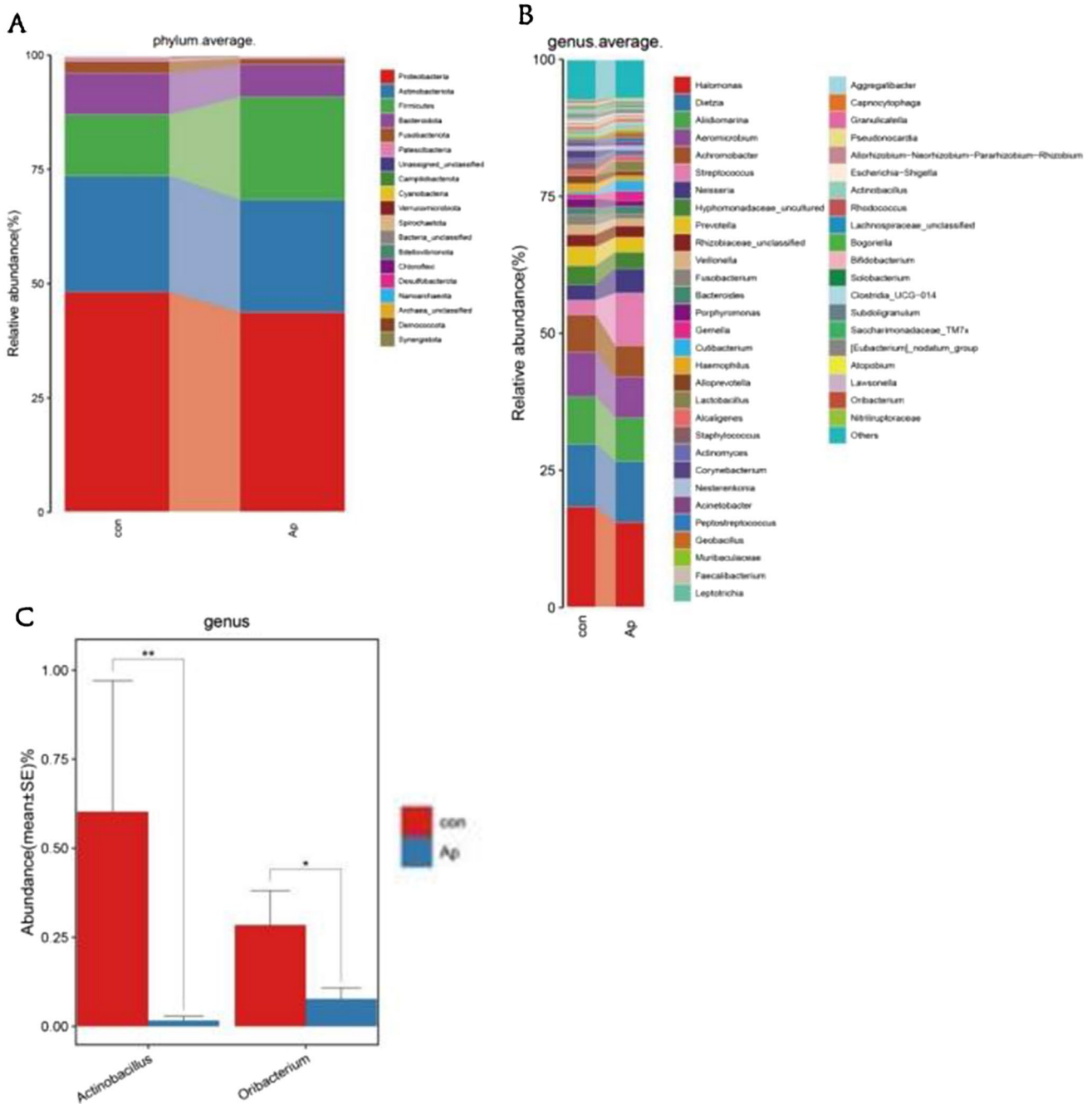


Fig. 4 Alterations in the microbiota of the duodenal mucosa in both groups. **A** Microbiota composition at the phylum level in the duodenal mucosa. **B** Microbiota composition at the genus level in the duodenal mucosa. **C** Differences in bacterial composition in the duodenal mucosa between the acute pancreatitis patients and healthy controls. Symbol * means $p < 0.05$, ** means $p < 0.01$, Mann–Whitney U tests

denal mucosa. **C** Differences in bacterial composition in the duodenal mucosa between the acute pancreatitis patients and healthy controls. Symbol * means $p < 0.05$, ** means $p < 0.01$, Mann–Whitney U tests

Plant_pathogen_interaction, and Environmental_adaptation were all significantly higher in the CON group than in the Ap group (Fig. 5C).

Discussion

AP is distinguished by an inflammatory cascade response that typically results in an overgrowth of intestinal bacteria, which exacerbates the disease by activating the innate immune system and bacterial translocation. The ileum is

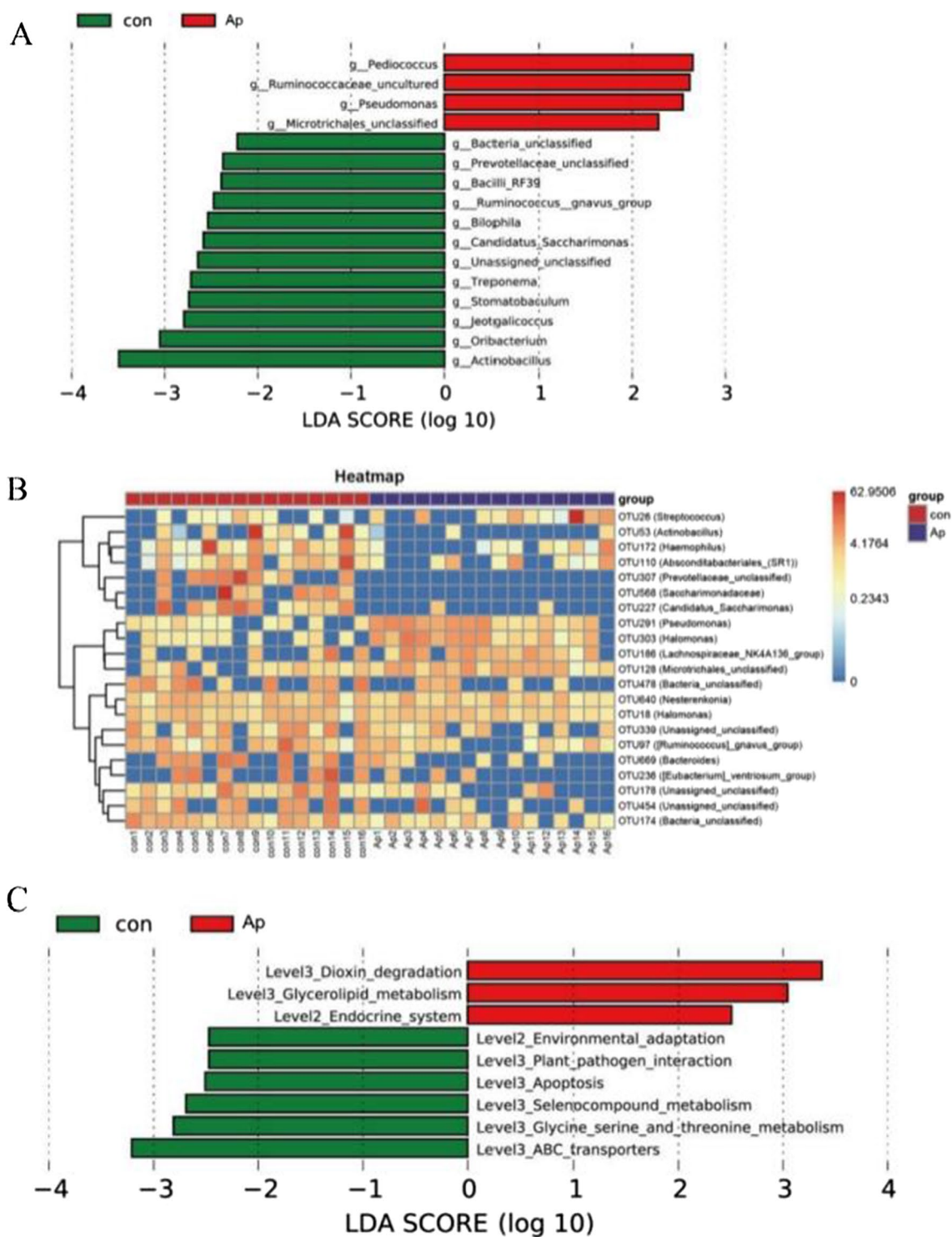


Fig. 5 Comparison of microbiome composition and Predictions of the functional alteration to the microbiota in both groups. **A** microbiota differences at the genus level, as assessed by Linear discriminant thought to have the most altered intestinal microbiota in acute pancreatitis [22]. Although research has shown that the displaced microbiota is from the small intestine, no research has been conducted to determine whether or not

analysis effect size. **B** A heatmap analysis of the microbiomes using a random forest model. **C** Predictions of the functional alteration to the microbiota of the duodenal mucosa in patients with acute pancreatitis the duodenal microbiota changes and how these changes affect disease [16]. In this study, we examined the mucosal microbiota of the descending duodenum and discovered that it changed slightly in acute pancreatitis.

The baseline characteristics of participants showed significantly elevated inflammatory factors in blood in the acute pancreatitis group. However, when we examined the morphological changes of the descending duodenum by pathology, the findings revealed no significant pathological damage to the descending duodenum in patients with acute pancreatitis compared to controls, including mucosal damage, inflammation, and hemorrhage/congestion. The intestinal mucosa normally serves as a barrier, we further tested the mucosal tight junction protein (Occludin and ZO-1) of the descending duodenum and it was discovered that acute pancreatitis impairs the duodenal barrier function.

Since intestinal damage can enhance mucosal permeability and bacterial translocation, we used 16S rRNA gene sequencing to examine the composition of the descending duodenum's mucosal microbiota in acute pancreatitis. The alpha diversity was not significantly different between the groups in this study; differences in microbiota between the two groups were detected by beta diversity and found to be different by the Adonis test based on unweighted UniFrac distances. It showed that the abundance of the mucosal microbiota of the descending duodenum had some slight changes in mild acute pancreatitis. This is consistent with a study that found no obvious change in the composition of the duodenal microbiota despite acute pancreatitis-induced duodenal bacterial overgrowth.

Further examination of the bacteriophage structure revealed that both groups primarily belonged to the *Proteobacteria* and *Actinobacteriota* phyla. Other researchers have reported similar results [26]. The dominant genera were roughly the same in both groups at the genus level, but the descending duodenal mucosa had higher levels of *Streptococcus* and *Neisseria* than the control group, and the healthy controls had higher levels of *Halothrix* and *Azithromycin*. *Streptococcus* and *Neisseria* are well-known pathogenic bacteria that have been linked to diseases such as meningitis and pneumonia. The Wilcoxon rank sum test revealed that *Actinobacillus* and *Oribacterium* were significantly different between the two groups, with both being more prevalent in the healthy control group.

There is no significant correlation between different genera and clinical inflammatory indicators using Spearman correlation analysis, which we think is because the duodenal mucosa in this investigation was collected from individuals with MAP. We speculate that changes in inflammatory markers and microbiota are more significant in SAP patients. We hypothesized that changes in inflammatory markers and microbiota are more significant in SAP patients, so we performed mouse experiments to confirm this. As a result, we examined the duodenum of healthy, MAP, and SAP mice and discovered that SAP mice had more serious duodenal mucosal damage than MAP and healthy mice. We

hypothesized that changes in duodenal mucosal microbiota were related to disease severity. In addition, the fact that the number of bacteria in the digestive tract gradually increases from top to bottom as the digestive tract progresses could explain this result to some extent. Because gastric juice contains a high concentration of digestive enzymes, the pH in the stomach is low, preventing intestinal bacteria from reproducing. The microbiota of the duodenum and stomach were essentially identical, but they contained coliform and anaerobic bacteria, whereas the abundance and diversity of microbiota in the jejunum, ileum, and colon increased gradually. This is also supported by the results of the current investigation, which found no significant inflammatory changes in the mucosal pathology of the duodenum after observing the mucosal pathology of the descending duodenum in acute pancreatitis. This speculation was also confirmed by this study, which found a gradual increase in the number of different genera along the gastrointestinal tract, based on alpha and beta diversity measurements. Moreover, this study found that the SAP duodenal mucosal microbiota showed a decrease in the genus *Alistipes* belonging to the phylum Bacteroidetes and an increase in the phylum Firmicutes including the genera *Romboutsia* and *Turicibacter* compared to the control group [19]. According to one study that investigated the microbiota of MAP and SAP mice, alterations in the microbiota were particularly noticeable in duodenal aspirates. However, the changes in gut microbiota composition were less pronounced in MAP compared to SAP. Furthermore, this study clarified that facultatively pathogenic bacteria such as *Escherichia/Shigella*, *Enterobacteriaceae* diversas, *Enterococcus*, and *Staphylococcus* were significantly enriched during SAP, which is also a sign of duodenal bacterial overgrowth [27].

There are several limitations to this study. For instance, the sample size was initially somewhat tiny. The possibility of statistically significant results could be achieved by increasing the sample size. Second, the duodenal mucosal microbiota was not tested in patients with severe acute pancreatitis, and the effect of disease severity on the microbiota was not validated in mice and human.

In conclusion, we demonstrate that minor damage to the duodenal mucosa occurs in MAP patients, as well as changes in the microbiota. We also found that the duodenal mucosal barrier was affected by disease severity by examining the duodenum of mice with varying disease severity. Although the relationship and mechanism between duodenal microbiota and AP remain to be confirmed, our research on duodenal mucosal microbiota extends the alteration of intestinal microbiota in acute pancreatitis and could be used as therapeutic targets in the future.

Supplementary Information The online version contains supplementary material available at <https://doi.org/10.1007/s10620-023-07948-8>.

Acknowledgments The authors would like to thank Chen H for her kind assistance and skilled technical assistance. Thanks to the Shanghai Natural Science Foundation Project (Grant No.22ZR1453500), the Science and Technology Project of Jiading Hospital, Shanghai General Hospital (Grant No. 202135A) and the Key Discipline Project of Shanghai Jiading District, Shanghai (2020-jdyxzdsk-15) for funding.

Author's contribution YL designed the research work. MC and MF performed the research activities. QJ conducted a statistical analysis. JW and MZ prepared figures and wrote the manuscript. MZ edited the manuscript submitted. All authors have read and given their approval for publication.

Funding This work was supported by the Shanghai Natural Science Foundation Project (Grant No.22ZR1453500), the Science and Technology Project of Jiading Hospital, Shanghai General Hospital (Grant No. 202135A) and the Key Discipline Project of Shanghai Jiading District, Shanghai (2020-jdyxzdsk-15).

Data availability The 16S rRNA sequence data generated in this study have been deposited in the Sequence Read Archive database under accession number PRJNA877061.

Declarations

Conflict of interest We confirm that there are no known conflicts of interest associated with this publication and there has been no significant financial support for this work that could have influenced its outcome. The authors declare no competing financial interests.

Ethical approval The studies involving humans and animals were reviewed and approved by the Clinical Center Laboratory Animal Welfare and Ethics committee of Shanghai First People's Hospital.

Open Access This article is licensed under a Creative Commons Attribution-NonCommercial 4.0 International License, which permits any non-commercial use, sharing, adaptation, distribution and reproduction in any medium or format, as long as you give appropriate credit to the original author(s) and the source, provide a link to the Creative Commons licence, and indicate if changes were made. The images or other third party material in this article are included in the article's Creative Commons licence, unless indicated otherwise in a credit line to the material. If material is not included in the article's Creative Commons licence and your intended use is not permitted by statutory regulation or exceeds the permitted use, you will need to obtain permission directly from the copyright holder. To view a copy of this licence, visit <http://creativecommons.org/licenses/by-nc/4.0/>.

References

- Beger HG, Rau BM. Severe acute pancreatitis: Clinical course and management. *World J Gastroenterol* 2007;13:5043–5051.
- Ammori BJ. Role of the gut in the course of severe acute pancreatitis. *Pancreas* 2003;26:122–129.
- Beger HG, Rau B, Isenmann R. Natural history of necrotizing pancreatitis. *Pancreatol* 2003;3:93–101.
- Schmid SW, Uhl W, Friess H et al. The role of infection in acute pancreatitis. *Gut* 1999;45:311–316.
- Clark JA, Coopersmith CM. Intestinal crosstalk: a new paradigm for understanding the gut as the “motor” of critical illness. *Shock* 2007;28:384–393.
- Pimentel M, Saad RJ, Long MD et al. ACG Clinical Guideline: Small Intestinal Bacterial Overgrowth. *Am J Gastroenterol* 2020;115:165–178.
- Gerritsen J, Timmerman HM, Fuentes S et al. Correlation between protection against sepsis by probiotic therapy and stimulation of a novel bacterial phylotype. *Appl Environ Microbiol* 2011;77:7749–7756.
- Van Felius ID, Akkermans LM, Bosscha K et al. Interdigestive small bowel motility and duodenal bacterial overgrowth in experimental acute pancreatitis. *Neurogastroenterol Motil* 2003;15:267–276.
- Bouhnik Y, Alain S, Attar A et al. Bacterial populations contaminating the upper gut in patients with small intestinal bacterial overgrowth syndrome. *Am J Gastroenterol* 1999;94:1327–1331.
- Zhang M, Zhu HM, He F et al. Association between acute pancreatitis and small intestinal bacterial overgrowth assessed by hydrogen breath test. *World J Gastroenterol* 2017;23:8591–8596.
- Liang XY, Jia TX, Zhang M. Intestinal bacterial overgrowth in the early stage of severe acute pancreatitis is associated with acute respiratory distress syndrome. *World J Gastroenterol* 2021;27:1643–1654.
- Li C, Zhu Y, Shenoy M et al. Anatomical and functional characterization of a duodeno-pancreatic neural reflex that can induce acute pancreatitis. *Am J Physiol Gastrointest Liver Physiol* 2013;304:G490–500.
- Futagami S, Wakabayashi M. Pancreatic Dysfunction and Duodenal Inflammatory Responses Coordinate with Refractory Epigastric Pain Including Functional Dyspepsia: A Narrative Review. *J Nippon Med Sch* 2022;89:255–262.
- Tan C, Ling Z, Huang Y et al. Dysbiosis of Intestinal Microbiota Associated With Inflammation Involved in the Progression of Acute Pancreatitis. *Pancreas* 2015;44:868–875.
- Zhu Y, He C, Li X et al. Gut microbiota dysbiosis worsens the severity of acute pancreatitis in patients and mice. *J Gastroenterol* 2019;54:347–358.
- Fritz S, Hackert T, Hartwig W et al. Bacterial translocation and infected pancreatic necrosis in acute necrotizing pancreatitis derives from small bowel rather than from colon. *Am J Surg* 2010;200:111–117.
- Samel S, Lanig S, Lux A et al. The gut origin of bacterial pancreatic infection during acute experimental pancreatitis in rats. *Pancreatol* 2002;2:449–455.
- Ma X, Huang L, Huang Z et al. The impacts of acid suppression on duodenal microbiota during the early phase of severe acute pancreatitis. *Sci Rep* 2020;10:20063.
- van den Berg FF, Hugenholtz F, Boermeester MA et al. Spatioregional assessment of the gut microbiota in experimental necrotizing pancreatitis. *BJS Open* 2021;5(5):zrab061.
- Leser TD, Molbak L. Better living through microbial action: the benefits of the mammalian gastrointestinal microbiota on the host. *Environ Microbiol* 2009;11:2194–2206.
- Sekirov I, Russell SL, Antunes LC et al. Gut microbiota in health and disease. *Physiol Rev* 2010;90:859–904.
- Chen J, Huang C, Wang J et al. Dysbiosis of intestinal microbiota and decrease in paneth cell antimicrobial peptide level during acute necrotizing pancreatitis in rats. *PLoS One* 2017;12:e0176583.
- Huang C, Chen J, Wang J et al. Dysbiosis of intestinal microbiota and decreased antimicrobial peptide level in paneth cells during hypertriglyceridemia-related acute necrotizing pancreatitis in rats. *Front Microbiol* 2017;8:776.
- Chiu CJ, McArdle AH, Brown R et al. Intestinal mucosal lesion in low-flow states. I. A morphological, hemodynamic, and metabolic reappraisal. *Arch Surg* 1970;101:478–483.

25. Schmidt J, Rattner DW, Lewandrowski K et al. A better model of acute pancreatitis for evaluating therapy. *Ann Surg* 1992;215:44–56.
26. Fan HN, Zhu P, Zhang J et al. Mucosal microbiome dysbiosis associated with duodenum bulb inflammation. *Microb Pathog* 2021;150:104711.
27. Glaubitz J, Wilden A, Frost F et al. Activated regulatory T-cells promote duodenal bacterial translocation into necrotic areas in severe acute pancreatitis [published online ahead of print, 2023 Jan 11]. *Gut*. 2023;gutjnl-2022–327448.

Publisher's Note Springer Nature remains neutral with regard to jurisdictional claims in published maps and institutional affiliations.